Published for SISSA by Springer

Received: April 20, 2022
Revised: August 10, 2022
Accepted: August 19, 2022
Published: September 16, 2022

Two-loop scattering amplitude for heavy-quark pair production through light-quark annihilation in QCD

Manoj K. Mandal,[a] **Pierpaolo Mastrolia,**[a,b] **Jonathan Ronca**[c] **and William J. Torres Bobadilla**[d]

[a] *INFN, Sezione di Padova, Via Marzolo 8, I-35131 Padova, Italy*
[b] *Dipartimento di Fisica e Astronomia, Università degli Studi di Padova, Via Marzolo 8, I-35131 Padova, Italy*
[c] *Dipartimento di Fisica, Università di Napoli Federico II, and INFN, Sezione di Napoli, Via Cinthia, I-80126 Napoli, Italy*
[d] *Max-Planck-Institut für Physik, Werner-Heisenberg-Institut, Föhringer Ring 6, D-80805 München, Germany*

E-mail: manojkumar.mandal@pd.infn.it, pierpaolo.mastrolia@unipd.it, ronca@na.infn.it, torres@mpp.mpg.de

Abstract: We present the first full analytic evaluation of the scattering amplitude for the process $q\bar{q} \to Q\bar{Q}$ up-to two loops in Quantum Chromodynamics, for a massless (q) and a massive (Q) quark flavour. The interference terms of the one- and two-loop amplitudes with the Born amplitude, decomposed in terms of gauge invariant form factors depending on the colour and flavour structure, are analytically calculated by keeping complete dependence on the squared center-of-mass energy, the squared momentum transfer, and the heavy-quark mass. The results are expressed as Laurent series around four space-time dimensions, with coefficients given in terms of generalised polylogarithms and transcendental constants up-to weight four. Our results validate the known, purely numerical calculations of the squared amplitude, and extend the analytic knowledge, previously limited to a subset of form factors, to their whole set, coming from both planar and non-planar diagrams, up-to the second order corrections in the strong coupling constant.

Keywords: Higher-Order Perturbative Calculations, Top Quark

ArXiv ePrint: 2204.03466

https://doi.org/10.1007/JHEP09(2022)129

JHEP09(2022)129

Contents

JHEP09(2022)129

1 Introduction

The production of top quark (t) and its anti-particle ($\bar{t}$) has been occupying a central role within the precision physics programme at hadron colliders, like the Tevatron and the Large Hadron Collider (LHC), over the last three decades. Being the heaviest known elementary particle, the t quark has offered a portal to the discovery of the Higgs boson, and it is considered pivotal for understanding the electroweak symmetry breaking mechanism. Studies of top-quark production (and decay) at the current LHC physics programme enters the high-precision tests of the parameters of the Standard Model (SM), such as couplings and masses, as well as the analyses of backgrounds, for discriminating deviations that could indicate the path to move beyond it. Within SM, the production of $t\bar{t}$ pairs in hadronic collisions is the main source of top quarks, therefore, it is considered among the cornerstone processes at the current and future hadron colliders. Because of its role for the precision physics programme at hadron colliders, the $t\bar{t}$-pair production has triggered a significant progress in the developments of theoretical methods for determination of the (differential) cross-sections, hence it has been stimulating the constant effort of providing calculations in Perturbative Quantum Chromodynamics (QCD), of increasing order in the strong-coupling series expansion.

The cross-section for $t\bar{t}$-production at LHC, at leading order (LO) and next-to-leading order (NLO) in QCD has been known since long [1–5]. The total cross section up-to the

next-to-next-to-leading order (NNLO) in QCD became available in [6–9]. Fully differential NNLO calculations require a major control over infrared (IR) divergences appearing at intermediate stages of the calculation. Partial results were obtained by using the antenna subtraction method [10–14]. The complete NNLO predictions were first carried out in [6–9, 15–18], by using the Stripper approach [19–21]. More recently, the NNLO computation of heavy-quark hadroproduction has been also completed in [22–26], within the q_T-subtraction scheme [27]. For recent studies on the strategies to perform precise higher-order computations in high-energy physics, see refs. [28, 29].

The calculation of the NNLO QCD corrections to $pp \to t\bar{t}$ requires four types of terms: the *double-real* corrections, coming from the tree-level squared amplitude for a process with two additional partons in the final state; the *real-virtual* corrections, due to the interference of the tree-level and of the one-loop amplitude for a process with one additional gluon in the final state; the *squared one-loop* corrections; the *double-virtual* corrections, due to the interference of the two-loop amplitude with the tree-level one.

The scattering amplitude for the real-virtual contributions were evaluated in [30, 31], and more recently in [32]. The purely virtual contributions depend on the square of one-loop amplitude and the genuine two-loop amplitude. The former has been computed analytically in [33–35], while the latter has been determined completely numerically in [36–38]. The analytic evaluation of the two-loop amplitude is known partially [39–44]. The main difficulty, in this case, is due to the analytic evaluation of the independent integrals appearing in the decomposition of the two-loop amplitudes, known as *master integrals* (MIs).

At parton-level, the $t\bar{t}$-production proceeds *via* the annihilation of a light-quark (q) and an anti-quark ($\bar{q}$), $q\bar{q} \to t\bar{t}$, and the more luminous gluon-fusion channel, $gg \to t\bar{t}$.

As regarding the gluon-fusion channel, the analytic evaluation of the interference of the two-loop amplitude with the tree-level amplitude is only partially complete, and they are expressed in terms of generalised polylogarithms (GPLs) and elliptic integrals [41–43, 45–47]. Very recently, the two-loop helicity amplitudes for the $t\bar{t}$-production in the gluon-fusion channel within the *leading colour approximation*, including the contribution of closed loops of quarks, has been computed in [44].

As regarding the light-quark pair annihilation channel, the interference of the two-loop amplitude with the corresponding tree-level amplitude can be decomposed in terms of ten form factors, according to the colour and flavour structure. Eight of them are known analytically, and expressed in terms of GPLs [39, 40, 48].

In this work, we present the complete analytic evaluation of the two-loop scattering amplitude for the scattering process $q\bar{q} \to Q\bar{Q}$, with a massless (q) and a massive (Q) quark flavour, in QCD, including leading and sub-leading colour contributions. We calculate the whole set of ten form factors analytically, including the two form factors previously unavailable, which take contribution from both planar and non-planar graphs. The latter do not contribute to the eight form factors already known, and their evaluation constitute part of the novel insights of the current work.

The loop integrals appearing in the un-renormalised interference terms of the one- and two-loop bare amplitudes with the leading-order one are regulated within the Conventional Dimensional Regularisation (CDR), where d is the number of continuous space-time dimensions.

JHEP09(2022)129

The calculation is automated within the AIDA [49] framework, implementing the adaptive integrand decomposition algorithm [50, 51] and interfaced: to FEYNARTS [52], FEYNCALC [53], for the automatic diagram generation and algebraic manipulations of the integrands; to REDUZE [54], and KIRA [55], for the generation of the relations required for the decomposition in terms of MIs; to SECDEC [56], for the numerical evaluation of MIs, if needed; to POLYLOGTOOLS [57], GINAC [58], and HANDYG [59], for the numerical evaluation of the analytic expressions. The cancellation of the ultraviolet (UV) divergences of the bare interference terms at one and two loops is carried out by renormalising the quark fields and masses in the *on-shell* scheme, and the strong coupling in the $\overline{\text{MS}}$-scheme, along the lines of [36, 39]. By using the analytic expressions of the MIs [39, 60–65], the renormalised interference terms are finally expressed as Laurent series around $d = 4$ dimensions, by keeping the complete dependence on the Mandelstam invariants s and t, and on the heavy-quark mass M. The one- and two-loop contributions are computed, respectively, up-to the first-order term, and up-to the finite term, in the four dimensional series expansion, whose coefficients are expressed in terms of GPLs and transcendental constants of up-to weight four. The analytic results are obtained in a non-physical region, where the variables s and t are negative, and are numerically continued to the physical region, above the heavy-quark pair-production threshold, $s \geq 4M^2$.

The structure of the infrared (IR) singularities of the massless and massive gauge theory scattering amplitudes has been studied in [66–76]. In the current work, the IR singularities of the two-loop renormalised amplitude are successfully compared to the predicted expression built within the Soft Collinear Effective Theory (SCET), along the lines of the method presented in [74, 76] and [77, 78].

The study of the virtual NNLO QCD corrections for the process $q\bar{q} \to Q\bar{Q}$, hereby presented, extends to the non-Abelian case the study of the four-fermion scattering amplitude with one massive fermion pair, in gauge theories, recently completed for the process $e^+ e^- \to \mu^+ \mu^-$ in Quantum Electrodynamics (QED) [79].

In the following pages, we describe the strategy we adopted to solve the problem of the analytic evaluation of the double-virtual NNLO corrections to one, out of two, partonic reactions contributing the hadroproduction of heavy-quark pair. Thus, providing what we consider an important validation and extension of the purely numerically known results, which have been employed to obtain state-of-the-art perturbative predictions within top-quark physics studies at hadron colliders (see [80–82] and reference therein, for recent applications).

2 Scattering amplitude

We consider the scattering amplitude of the process,

$$q(p_1) + \bar{q}(p_2) \to Q(p_3) + \bar{Q}(p_4)\,, \tag{2.1}$$

where q [$\bar{q}$] stands for a massless quark [anti-quark], i.e. $m_q = 0$, and Q [$\bar{Q}$], for a massive quark [anti-quark], i.e. $m_Q = M \neq 0$, in QCD. The Mandelstam invariants of the scattering

JHEP09(2022)129

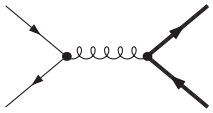

Figure 1. Tree-level Feynman diagrams for the process $q\bar{q} \to Q\bar{Q}$. Thin lines indicate a light quark (q), whilst thick ones indicate a heavy quark (Q); curly lines correspond to gluons.

reaction are $s = (p_1 + p_2)^2$, $t = (p_1 - p_3)^2$, and $u = (p_2 - p_3)^2$, satisfying the condition $s + t + u = 2M^2$. In the physical region, the range of Mandelstam variables reads,

$$s \geq 4M^2 \quad \& \quad -\left(\frac{\sqrt{s} - \sqrt{s-4M^2}}{2}\right)^2 \leq t \leq -\left(\frac{\sqrt{s} + \sqrt{s-4M^2}}{2}\right)^2 . \tag{2.2}$$

The dependence of the scattering amplitude on the kinematic variables can be conveniently parametrised in terms of the dimensionless variables, η and ϕ, defined as,

$$\eta = \frac{s}{4M^2} - 1 , \qquad \phi = \frac{M^2 - t}{s} , \tag{2.3}$$

which, in the physical region satisfy the conditions,

$$\eta > 0 \quad \& \quad \frac{1}{2}\left(1 - \sqrt{\frac{\eta}{1+\eta}}\right) \leq \phi \leq \frac{1}{2}\left(1 + \sqrt{\frac{\eta}{1+\eta}}\right) . \tag{2.4}$$

The scattering amplitude $\mathcal{A}$ of the process can be evaluated in perturbative QCD, and expressed as a power series in the strong coupling α_s, as,

$$\mathcal{A}(\alpha_s) = 4\pi\alpha_s \left[\mathcal{A}^{(0)} + \left(\frac{\alpha_s}{\pi}\right)\mathcal{A}^{(1)} + \left(\frac{\alpha_s}{\pi}\right)^2 \mathcal{A}^{(2)} + \mathcal{O}\left(\alpha_s^3\right)\right] . \tag{2.5}$$

The LO term $\mathcal{A}^{(0)}$, referred to as *Born term*, receives contribution from a single tree-level Feynman diagram, see figure 1. The colour-summed, un-polarised squared amplitude at LO (summed over the number of colours, summed over the final spins, and averaged over the initial states) has a rather simple expression,

$$\mathcal{M}^{(0)} = \frac{1}{4} \sum_{\substack{\text{colours} \\ \text{spins}}} |\mathcal{A}^{(0)}|^2 = \left(N_c^2 - 1\right) A^{(0)} , \tag{2.6}$$

with,

$$A^{(0)} = \frac{2(1-\epsilon)s^2 + 4\left(t - M^2\right)^2 + 4st}{s^2} , \tag{2.7}$$

where N_c is the number of colours, and $\epsilon = (4-d)/2$, with d being the number of (continuous) space-time dimensions. The higher order contributions $\mathcal{A}^{(n)}$, with $n = 1, 2$, get contributions from one- and two-loop diagrams, respectively, shown in figures 2 and 3, 4. The interferences of one- and two-loop amplitudes with the Born term are defined as,

$$\mathcal{M}^{(n)} = \frac{1}{4} \sum_{\substack{\text{colours} \\ \text{spins}}} 2\,\mathrm{Re}(\mathcal{A}^{(0)*}\,\mathcal{A}^{(n)}) , \text{ for } n = 1, 2 , \tag{2.8}$$

JHEP09(2022)129

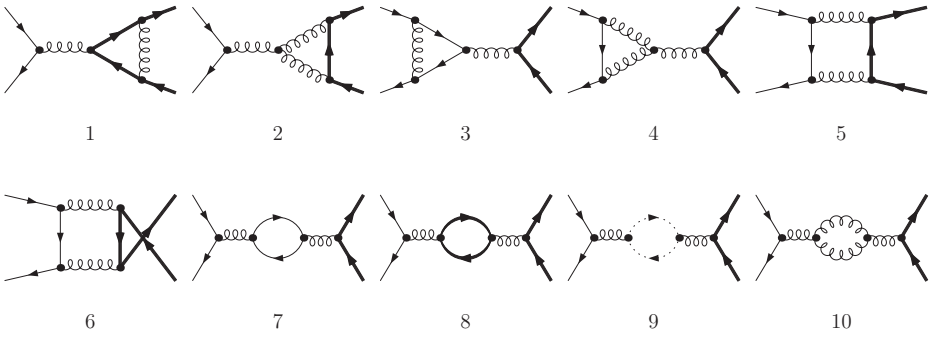

Figure 2. One-loop Feynman diagrams for the process $q\bar{q} \to Q\bar{Q}$. Thin lines indicate a light quark (q), whilst thick ones indicate a heavy quark (Q); curly and dashed lines correspond to gluons and ghosts, respectively.

and can be organised as combinations of gauge invariant factors, according to the dependence on the number of colours (N_c) and on the flavour structure (i.e., the number of light- and heavy-fermion closed loops, respectively, n_l and n_h). In particular, the contributions at one- and two-loop admit the following decomposition [36, 37, 48],

$$\mathcal{M}^{(1)} = 2\left(N_c^2 - 1\right)\left(A^{(1)}\, N_c + \frac{B^{(1)}}{N_c} + C_l^{(1)}\, n_l + C_h^{(1)}\, n_h\right), \tag{2.9}$$

$$\begin{aligned}\mathcal{M}^{(2)} = 2\left(N_c^2 - 1\right)\Bigg(&A^{(2)}\, N_c^2 + B^{(2)} + \frac{C^{(2)}}{N_c^2} + D_l^{(2)}\, N_c\, n_l + D_h^{(2)}\, N_c\, n_h \\ &+ E_l^{(2)}\frac{n_l}{N_c} + E_h^{(2)}\frac{n_h}{N_c} + F_l^{(2)}\, n_l^2 + F_{lh}^{(2)}\, n_l\, n_h + F_h^{(2)}\, n_h^2\Bigg).\end{aligned} \tag{2.10}$$

The analytic expressions of the one-loop form factors have been known since long time [1–5, 83–85].

Regarding the two-loop form factors in the colour decomposition (2.10), contributions from the *leading colour* ($A^{(2)}$), one closed fermionic loop ($D_l^{(2)}$, $D_h^{(2)}$, $E_l^{(2)}$, $E_h^{(2)}$), and two closed fermionic loops ($F_l^{(2)}, F_{lh}^{(2)}, F_h^{(2)}$) are known both numerically as well as analytically [36, 39, 40]; $B^{(2)}$ and $C^{(2)}$, instead, are known only numerically [36]. Their analytic evaluation requires the evaluation of non-planar diagrams (that give no contribution to the leading colour term), and they are presented for the first time in this work.

The evaluation of the previously known colour factors, together with the novel calculation of $B^{(2)}$ and $C^{(2)}$, allows us to obtain, for the first time, the complete analytic expression of the two-loop scattering amplitude for the four-quark scattering in QCD with a massive quark-pair, both as internal and as external states.

The results for the four-quark scattering $q\bar{q} \to Q\bar{Q}$ in QCD, hereby presented, can be considered as the natural extension to a non-Abelian theory of the ones obtained for the four-fermion scattering $e^+e^- \to \mu^+\mu^-$ in QED, recently presented in [79]. We observe that the coefficient $C^{(2)}$, as well as $E_l^{(2)}, E_h^{(2)}$, $F_l^{(2)}, F_{lh}^{(2)}$, and $F_h^{(2)}$, can be written as linear combination of (colour stripped) Feynman diagrams that appear also in the Abelian case. The form factors $A^{(2)}$, $B^{(2)}$, $D_l^{(2)}$, and $D_h^{(2)}$ get contribution from Abelian and non-Abelian

JHEP09(2022)129

(colour stripped) diagrams. We refer the Reader to appendix A for a detailed discussion on the colour decomposition.

The complete analytic calculation of $\mathcal{M}^{(2)}$, or in other words, the computation of the form factors in decomposition (2.10), is the main result of the present manuscript.

3 Analytic evaluation

We begin by considering the bare LO squared amplitude and the bare interference terms,

$$\mathcal{M}_{\rm b}^{(0)} = \frac{1}{4} \sum_{\substack{\text{colours} \\ \text{spins}}} |\mathcal{A}_{\rm b}^{(0)}|^2 \,, \tag{3.1}$$

$$\mathcal{M}_{\rm b}^{(n)} = \frac{1}{4} \sum_{\substack{\text{colours} \\ \text{spins}}} 2\,\text{Re}(\,\mathcal{A}_{\rm b}^{(0)*}\,\mathcal{A}_{\rm b}^{(n)}\,)\,, \text{ for } n = 1, 2\,, \tag{3.2}$$

where $\mathcal{A}_{\rm b}^{(n)}$ $(n \geq 0)$ are the coefficients of the series expansion of the bare amplitude $\mathcal{A}_{\rm b}$ in the bare strong coupling constant, $\alpha_s^{\rm b} \equiv g_s^2/(4\pi)$. Its expression up-to the second-order corrections reads as,

$$\mathcal{A}_{\rm b}\left(\alpha_s^{\rm b}\right) = 4\pi\alpha_s^{\rm b}\, S_\epsilon\, \mu^{-2\epsilon} \left[\mathcal{A}_{\rm b}^{(0)} + \left(\frac{\alpha_s^{\rm b}}{\pi}\right) \mathcal{A}_{\rm b}^{(1)} + \left(\frac{\alpha_s^{\rm b}}{\pi}\right)^2 \mathcal{A}_{\rm b}^{(2)} + O\Big((\alpha_s^{\rm b})^3\Big)\right], \tag{3.3}$$

with $S_\epsilon \equiv (4\pi e^{-\gamma_E})^\epsilon$, and μ being the 't Hooft mass scale. The CDR scheme is adopted throughout the whole computation, hence, internal and external states are, accordingly, regularised in $d = 4 - 2\epsilon$ space-time dimensions [86–88]. The LO term $\mathcal{A}_{\rm b}^{(0)} = \mathcal{A}^{(0)}$, given in eq. (2.6), is finite in the limit $d \to 4$ $(\epsilon \to 0)$; whereas the higher order terms require the evaluation of one- and two-loop integrals that may contain UV and IR divergences, parametrised as poles in ϵ.

3.1 UV renormalisation

The one- and two-loop amplitudes contain both UV and IR divergences. The UV divergences are removed by renormalising the bare quark fields and the bare mass of the heavy quark in the on-shell scheme,

$$\psi_{\rm b} = \sqrt{Z_2}\,\psi\,, \quad M_{\rm b} = Z_M M\,, \tag{3.4}$$

and by renormalising the bare coupling constant $\alpha_s^{\rm b}$ at the scale μ in the $\overline{\rm MS}$ scheme,

$$\alpha_s^{\rm b}\, S_\epsilon = \alpha_s(\mu^2)\, \mu^{2\epsilon}\, Z_{\alpha_s}^{\overline{\rm MS}}\,. \tag{3.5}$$

By employing this, we can express the renormalised amplitude in terms of the bare amplitude as,

$$\mathcal{A} = Z_{2,q}\, Z_{2,Q}\, \mathcal{A}_{\rm b}\Big(\alpha_s^{\rm b} = \alpha_s^{\rm b}(\alpha_s)\,, M_{\rm b} = M_{\rm b}(M)\Big)\,, \tag{3.6}$$

where $Z_{2,q}$ and $Z_{2,Q}$ are the on-shell wave function renormalisation constants for the massless and massive quarks; M is the renormalised mass for the heavy quark in the

JHEP09(2022)129

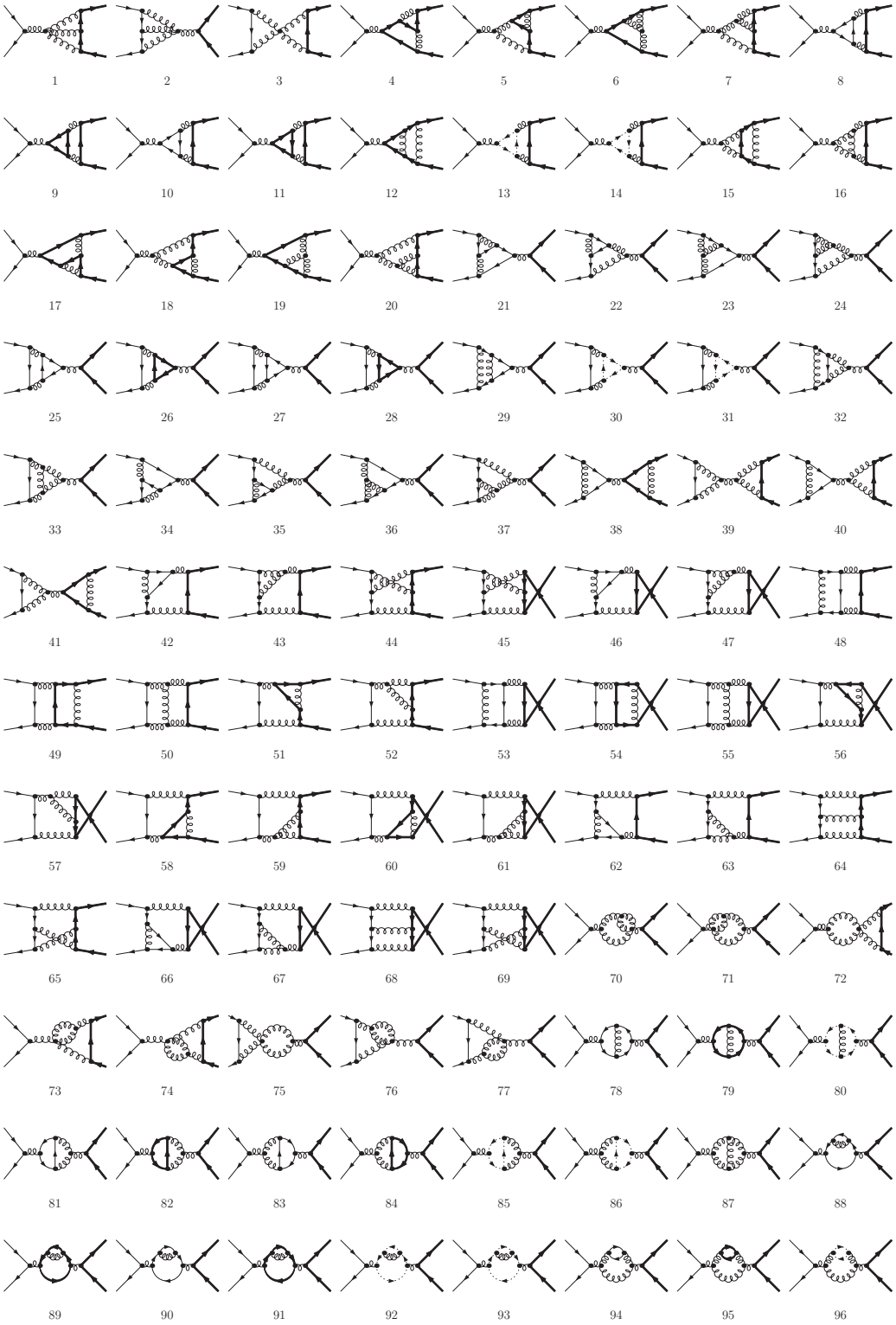

Figure 3. Two-loop Feynman diagrams for the process $q\bar{q} \to Q\bar{Q}$ (set 1 of 2).

JHEP09(2022)129

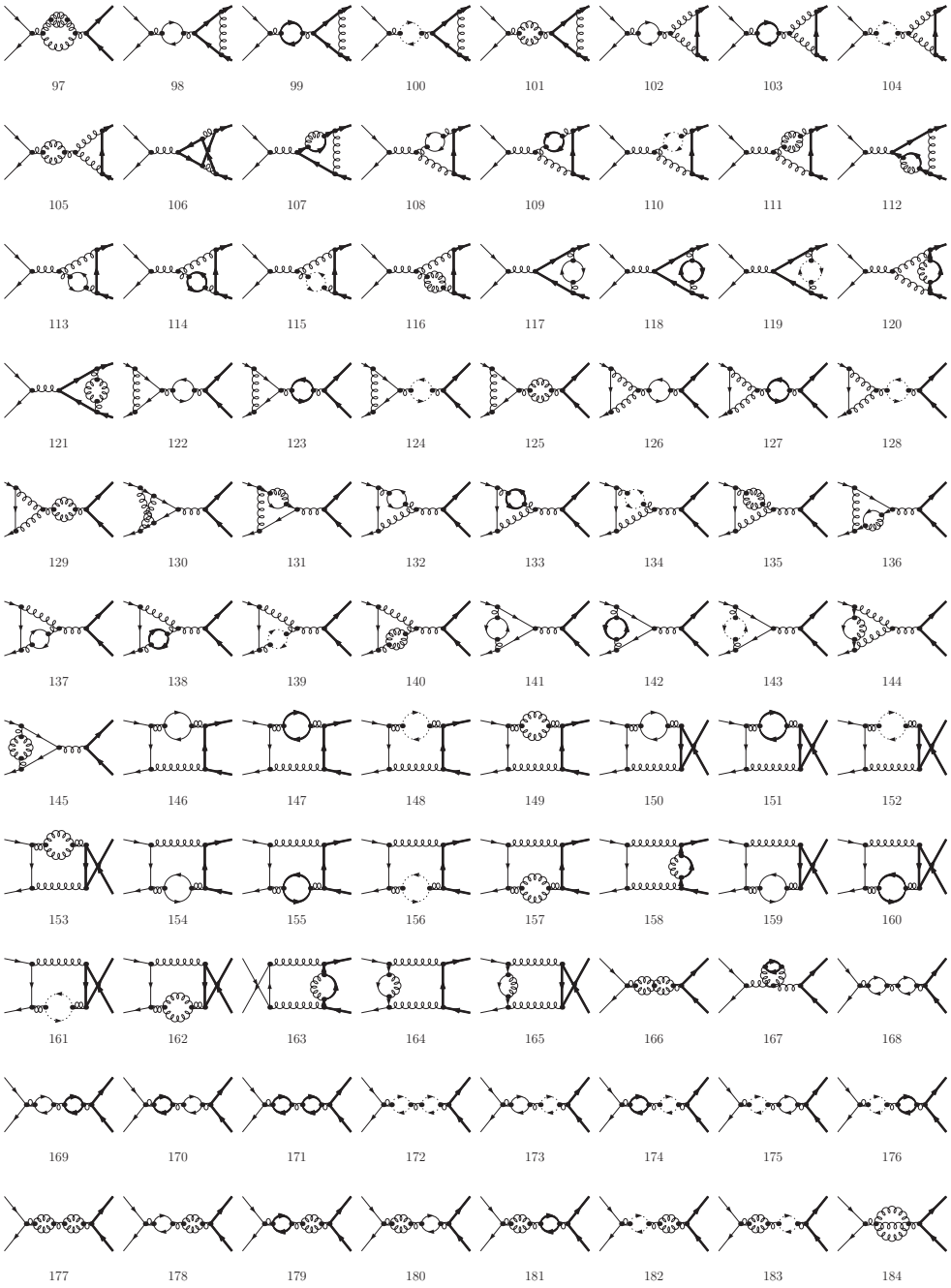

Figure 4. Two-loop Feynman diagrams for the process $q\bar{q} \to Q\bar{Q}$ (set 2 of 2).

on-shell scheme. The renormalised amplitude depends on four renormalisation constants $(Z_{2,q}, Z_{2,Q}, Z_{\alpha_s}, Z_M)$, which admit a perturbative expansion in the renormalised coupling constant α_s,

$$Z_j = 1 + \left(\frac{\alpha_s}{\pi}\right) \delta Z_j^{(1)} + \left(\frac{\alpha_s}{\pi}\right)^2 \delta Z_j^{(2)} + \mathcal{O}(\alpha_s^3)\,, \quad \text{for } j = \{q, Q, \alpha_s, M\}\,. \tag{3.7}$$

JHEP09(2022)129

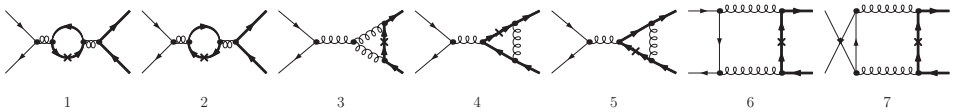

Figure 5. Mass renormalisation counter-term diagrams.

The mass and wave-function renormalisation of the heavy quark is known to three loop accuracy in the on-shell scheme [89–91]; the wave-function renormalisation of the light quark, due to the presence of heavy quark, is provided at two loop accuracy in [48]; the strong coupling constant renormalisation is known up-to five-loop accuracy [92–97]. Their expressions, up-to the required order, are collected in appendix B.

Upon combining eqs. (3.3), (3.6), and (3.7), we obtain the UV renormalised amplitude $\mathcal{A}$, given in eq. (2.5), whose coefficients $\mathcal{A}^{(n)}$ can be written in terms of the bare coefficients $\mathcal{A}_{\rm b}^{(n)}$, as,

$$\mathcal{A}^{(0)} = \mathcal{A}_{\rm b}^{(0)}, \qquad \mathcal{A}^{(n)} = \mathcal{A}_{\rm b}^{(n)} + \delta\mathcal{A}^{(n)}\,, \quad (n>0)\,, \tag{3.8}$$

with,

$$\delta\mathcal{A}^{(1)} = \Big(\delta Z_{\alpha_s}^{(1)} + \delta Z_Q^{(1)}\Big)\mathcal{A}_{\rm b}^{(0)}, \tag{3.9a}$$

$$\delta\mathcal{A}^{(2)} = \Big(2\delta Z_{\alpha_s}^{(1)} + \delta Z_Q^{(1)}\Big)\mathcal{A}_{\rm b}^{(1)} + \Big(\delta Z_{\alpha_s}^{(2)} + \delta Z_Q^{(2)} + \delta Z_q^{(2)} + \delta Z_Q^{(1)}\delta Z_{\alpha_s}^{(1)}\Big)\mathcal{A}_{\rm b}^{(0)} + \delta Z_M^{(1)}\mathcal{A}_{\rm b}^{(1,\text{mass CT})}\,. \tag{3.9b}$$

The last term in eq. (3.9b), corresponding to the mass renormalisation counter-term, takes contributions from the diagrams depicted in figure 5 and consists of the one-loop diagrams with an insertion of the mass counter-term in the heavy-quark propagators.

With the above definitions, one- and two-loop renormalised interference terms $\mathcal{M}^{(n)}$ are obtained as,

$$\mathcal{M}^{(n)} = \mathcal{M}_{\rm b}^{(n)} + \delta\mathcal{M}^{(n)}\,, \qquad \text{for } n=1,2\,, \tag{3.10}$$

where,

$$\delta\mathcal{M}^{(n)} = \frac{1}{4}\sum_{\substack{\text{colours}\\ \text{spins}}} 2\,\text{Re}\Big(\mathcal{A}_{\rm b}^{(0)*}\,\delta\mathcal{A}^{(n)}\Big)\,. \tag{3.11}$$

3.2 Algebraic decomposition

The generation of the one- and two-loop diagrams contributing to $\mathcal{M}_{\rm b}^{(1)}$ and $\mathcal{M}_{\rm b}^{(2)}$, as well as of those needed for the mass-renormalisation, is carried out using FeynArts [52]. By choosing Feynman gauge for the gluon propagator, we identify 10 diagrams at one loop, 184 diagrams at two loops, and 7 counter-term diagrams for the mass renormalisation, respectively, shown in figure 2, figures 3 and 4, and figure 5. Scaleless loop integrals (e.g., one- and two-loop massless tadpoles), and non-planar diagrams that vanish because of colour algebra (see figure 6) are neglected.[1]

[1]Details on the diagrammatic contributions to the colour decomposition can be found in appendix A.

JHEP09(2022)129

Figure 6. Two-loop diagrams that, upon interference with the Born amplitude, give rise to vanishing contributions, due to colour algebra.

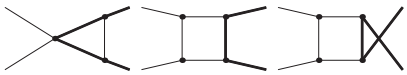

Figure 7. One-loop parent graphs for the process $q\bar{q} \to Q\bar{Q}$. Thin lines indicate massless propagators, whilst thick ones indicate massive ones.

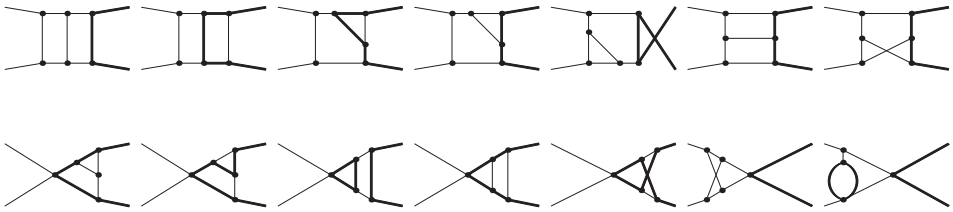

Figure 8. Representative two-loop parent graphs for the process $q\bar{q} \to Q\bar{Q}$. Thin [Thick] lines indicate massless [massive] particles.

After performing colour, spin and Dirac-γ algebra by means of FeynCalc [53], the interference terms are expressed in terms of n-loop scalar integrals as,

$$\mathcal{M}_{\rm b}^{(n)} = (S_\epsilon)^n \int \prod_{i=1}^{n} \frac{d^d k_i}{(2\pi)^d} \sum_G \frac{N_G(p_i, k_i, M^2)}{\prod_{\sigma \in G} D_\sigma(p_i, k_i, M^2)} \quad , \tag{3.12}$$

where G denotes an n-loop graph interfered with the Born terms, D_σ denotes the set of denominators corresponding to the internal lines of G, and N_G stands for a polynomial in the scalar products built out of external momenta p_i and loop momenta k_i, and M^2.

The decomposition of the integrals is automated within the Aida framework [49], where integrands are grouped according to their common set of propagators with respect to the ones of the parent graphs, identified among all the diagrams as the ones with the largest sets of independent denominators. At one-loop, Aida identifies 3 parent graphs, shown in figure 7; at two-loop, 31 parent diagrams (22 belonging to four-point topologies and 9 belonging to three-point topologies), shown in figure 8, for representative topologies.

The quantities $\mathcal{M}^{(n)}$ are simplified within Aida by employing the *adaptive integrand decomposition method* [50, 51] followed by the use of *integration-by-parts identities* [98–100]. The latter are automatically generated for the parent diagrams only, generated by Aida through its interface to the public codes Reduze [54] and Kira [55]. After integrand and integral decompositions, the interference terms $\mathcal{M}_{\rm b}^{(n)}$ appear to be written as linear combinations of a set of independent MIs, say $\mathbf{I}^{(n)}$,

$$\mathcal{M}_{\rm b}^{(n)} = \mathbb{C}^{(n)} \cdot \mathbf{I}^{(n)} \,, \tag{3.13}$$

where $\mathbb{C}^{(n)}$ represents a vector of coefficients, rational functions depending on ϵ and the kinematic variables, s, t, M^2. In particular, at one-loop, $\mathbf{I}^{(1)}$ is a vector of 12 MIs, and, at

JHEP09(2022)129

two-loop, $\mathbf{I}^{(2)}$ is a vector of 270 MIs, analytically known: two- and three-point functions, and a subset of the planar four-point functions have been known since long [39, 40, 60–62], whereas the complete set of planar and non-planar four-point integrals were computed in [63, 64, 101][2] using the differential equation method via Magnus exponential [103], and independently in [65].

The one-loop counter-term $\delta\mathcal{M}^{(1)}$ is directly computed from the knowledge of the renormalisation constants δZ_j and the Born squared amplitude. Differently, the two-loop counter-term $\delta\mathcal{M}^{(2)}$ requires also the decomposition of one-loop integrals, due to both the genuine one-loop amplitude and to the mass renormalisation counter-term, coming from the one-loop diagrams shown in figure 5, and, therefore, it admits a decomposition in terms of the basis $\mathbf{I}^{(1)}$.

4 Results

After inserting the expression of the MIs and adding the bare quantities $\mathcal{M}_{\rm b}^{(n)}$ to the corresponding counter-terms $\delta\mathcal{M}^{(n)}$, finally, the renormalised interference terms $\mathcal{M}^{(n)}$ are analytically expressed as a Laurent series around $\epsilon = 0$, as

$$\mathcal{M}^{(1)} = \sum_{k=-2}^{1} \mathcal{M}_k^{(1)}\,\epsilon^k + \mathcal{O}(\epsilon^2)\,, \qquad \text{and} \quad \mathcal{M}^{(2)} = \sum_{k=-4}^{0} \mathcal{M}_k^{(2)}\,\epsilon^k + \mathcal{O}(\epsilon)\,, \tag{4.1}$$

whose coefficients $\mathcal{M}_k^{(n)}$ contain GPLs, iteratively defined as [104],

$$G(w_n,\ldots,w_1;\tau) \equiv \int_0^\tau \frac{dt}{t-w_n} G(w_{n-1},\ldots,w_1;t)\,, \tag{4.2a}$$

$$\text{with} \quad G(w_1;\tau) \equiv \log\left(1-\frac{\tau}{w_1}\right). \tag{4.2b}$$

The analytical expression of $\mathcal{M}^{(1)}$ and $\mathcal{M}^{(2)}$ are computed in the non-physical region, $s<0$, $t<0$, and their analytic continuation to the region of heavy-quark pair production is performed numerically. In particular, $\mathcal{M}^{(2)}$ contains 5033 GPLs up-to weight four, whose arguments are written in terms of 18 letters, $w_i = w_i(x,y,z)$ defined as,

$$\begin{aligned}
w_1 &= x\,, & w_2 &= 1+x\,,\\
w_3 &= 1-x\,, & w_4 &= y\,,\\
w_5 &= 1+y\,, & w_6 &= 1-y\,,\\
w_7 &= x+y\,, & w_8 &= 1+xy\,,\\
w_9 &= 1-y(1-x-y)\,, & w_{10} &= z\,,\\
w_{11} &= 1+z\,, & w_{12} &= 1-z\,,\\
w_{13} &= z+y\,, & w_{14} &= z-y\,,\\
w_{15} &= z^2-y\,, & w_{16} &= 1-y+y^2-z^2\,,\\
w_{17} &= 1-3y+y^2+z^2\,, & w_{18} &= z^2-y^2-yz^2+y^2z^2\,,
\end{aligned} \tag{4.3}$$

[2] A comparison on a planar subset of master integrals, computed both in [39] and in [63], partly performed along the lines of [102], revealed that the numerical coefficient (a rational number) of π^4, within the weight-four term of the integrals I_{30} and I_{31}, defined in eq. (6.2) of [63], was not correct. The revised version of the corresponding ancillary file, containing the analytic expression of the planar set of MIs used in this work, is available on the arXiv.

JHEP09(2022)129

which depend on the Mandelstam variables through the relations [63, 64, 101],

$$-\frac{t}{M^2} = x, \quad -\frac{s}{M^2} = \frac{(1-y)^2}{y}, \quad -\frac{u-M^2}{t-M^2} = \frac{z^2}{y}\,, \tag{4.4}$$

and their inverse,

$$x = -\frac{t}{M^2}, \quad y = \frac{(2M^2 - s - \sqrt{4M^2 - s}\,\sqrt{-s})}{2M^2}, \quad z = \frac{\sqrt{y}\,\sqrt{u-M^2}}{\sqrt{M^2-t}}\,. \tag{4.5}$$

The numerical evaluation of GPLs, in the physical region (2.4), is performed by adopting the prescription,

$$s \to s + i\delta\,, \tag{4.6}$$

by assigning a small positive imaginary part to the squared center-of-mass energy variable, above the pair production threshold.[3]

As anticipated in section 2, the analytic evaluation of the one-loop amplitude has been performed long ago by following different approaches [1–5, 83–85]. On the two-loop side, instead, analytic expressions for the form factors present in the colour decomposition (2.10) is partially known. In particular, the knowledge of these analytic expressions is restricted to leading-colour and closed fermion-loop terms ($A^{(2)}$, $D_l^{(2)}$, $D_h^{(2)}$, $E_l^{(2)}$, $E_h^{(2)}$, $F_l^{(2)}, F_{lh}^{(2)}, F_h^{(2)}$) [39, 40]. The analytic evaluation of $B^{(2)}$ and $C^{(2)}$ required the evaluation of non-planar diagrams, that were absent from the leading-colour term, and they are presented for the first time in this work.

The independent evaluation of the previously known form factors, together with the novel calculation of $B^{(2)}$ and $C^{(2)}$, allows us to validate the previously known numerical results [36], and to obtain, for the first time, the complete analytic expression of the two-loop scattering amplitude for the partonic scattering $q\bar{q} \to Q\bar{Q}$ in QCD. Our result is the first example of a complete analytic calculation of a two-loop amplitude in QCD with a massive quark-pair in the internal and as well as external states, including both the leading and sub-leading colour contributions.

The analytic expressions are too long to be shown here, therefore, we provide them in a Mathematica notebook file, available at:

https://wjtorresb@bitbucket.org/wjtorresb/interfamp_ttbar.git

For the convenience of the users, we include two Mathematica notebook files to numerically evaluate the expression at a specific phase-space point with the aid of HandyG [59] and Ginac [58] through PolyLogTools [57].

A flow chart of the complete computational algorithm implemented in the Aida package is shown in figure 9.

[3]The numerical effect of $\delta \neq 0$ has been estimated to be of $\mathcal{O}(\delta)$, therefore, yielding numerical values of the interference terms in double precision with a choice of $\delta \sim \mathcal{O}(10^{-17})$.

JHEP09(2022)129

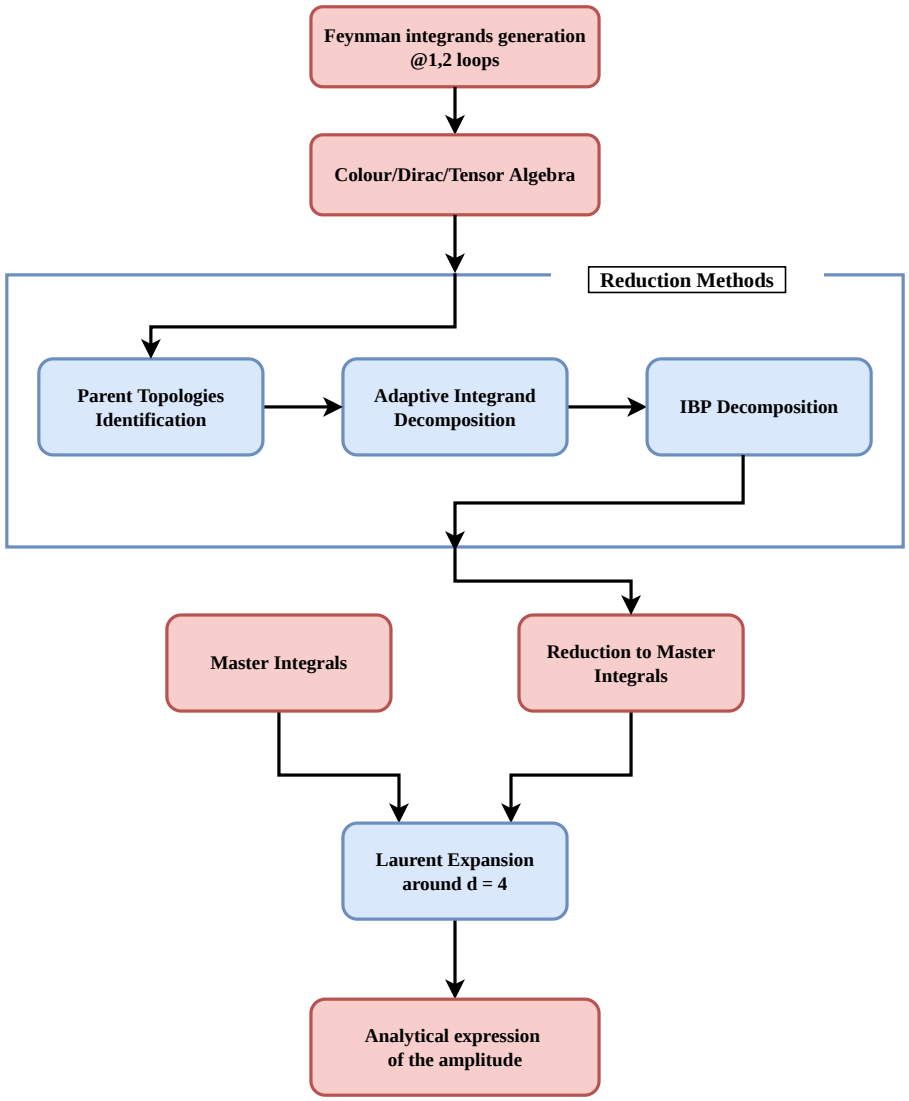

Figure 9. Flow-chart of the AIDA framework.

4.1 IR structure

The structure of IR singularities of the massless and massive gauge theory scattering amplitudes has been studied in [66–76]. The coefficients of the poles in ϵ appearing in the renormalised amplitudes $\mathcal{M}^{(1)}$ and $\mathcal{M}^{(2)}$ agree with the the universal IR structures of the QCD amplitudes, derived from the knowledge of the lower order terms, within SCET [74, 76–78, 105],

$$\sum_{k=-2}^{-1} \mathcal{M}_k^{(1)}\,\epsilon^k = 2Z_1^{\rm IR}\,\mathcal{M}^{(0)}\Big|_{\rm poles}\,, \tag{4.7a}$$

$$\sum_{k=-4}^{-1} \mathcal{M}_k^{(2)}\,\epsilon^k = 2\Big[\Big(Z_2^{\rm IR} - \big(Z_1^{\rm IR}\big)^2\Big)\,\mathcal{M}^{(0)} + \frac{1}{2}\,Z_1^{\rm IR}\,\mathcal{M}^{(1)}\Big]\Big|_{\rm poles}\,, \tag{4.7b}$$

JHEP09(2022)129

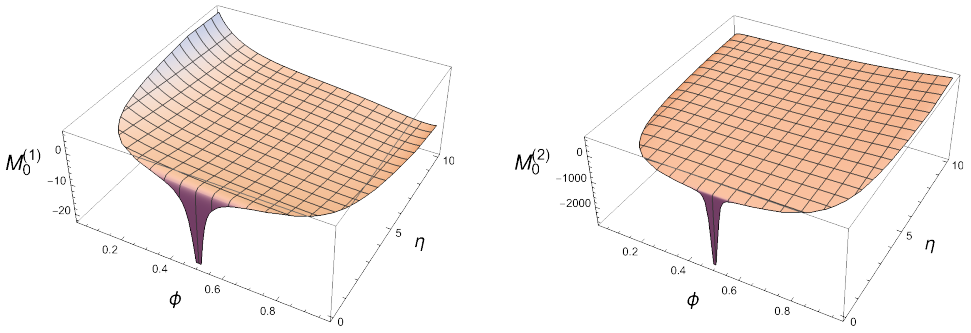

Figure 10. Three-dimensional plots of the finite terms $\mathcal{M}_0^{(n)}$, $n = 1, 2$, of the renormalised one- and two-loop amplitudes, in eqs. (2.9), (2.10), where $N_c = 3, n_l = 5$, and $n_h = 1$.

where $Z_i^{\rm IR}$ $(i = 1, 2)$ are the coefficients of the IR renormalisation factor $\boldsymbol{Z}_{\rm IR}$ encoding the IR divergence. For the process under consideration, involving the production of a massive quark pair, $\boldsymbol{Z}_{\rm IR}$ reads as [78],

$$\boldsymbol{Z}_{\rm IR} = 1 + \left(\frac{\alpha_s}{\pi}\right) Z_1^{\rm IR} + \left(\frac{\alpha_s}{\pi}\right)^2 Z_2^{\rm IR} + \mathcal{O}(\alpha_s^3)\,, \tag{4.8}$$

with,

$$Z_1^{\rm IR} = \frac{\Gamma_0'}{16\epsilon^2} + \frac{\boldsymbol{\Gamma}_0}{8\epsilon}\,, \tag{4.9}$$

$$\begin{aligned} Z_2^{\rm IR} = {} & \frac{(\Gamma_0')^2}{512\epsilon^4} + \frac{\Gamma_0'}{128\epsilon^3}\left(\boldsymbol{\Gamma}_0 - \frac{3}{2}\beta_0\right) + \frac{\boldsymbol{\Gamma}_0}{128\epsilon^2}(\boldsymbol{\Gamma}_0 - 2\beta_0) + \frac{\Gamma_1'}{256\epsilon^2} + \frac{\boldsymbol{\Gamma}_1}{64\epsilon} \\ & - \frac{2\,T_F}{3}\sum_{i=1}^{n_h}\left[\frac{\Gamma_0'}{16}\left(\frac{1}{2\epsilon^2}\ln\frac{\mu^2}{m_i^2} + \frac{1}{4\epsilon}\left[\ln^2\frac{\mu^2}{m_i^2} + \frac{\pi^2}{6}\right]\right) + \frac{\boldsymbol{\Gamma}_0}{16\epsilon}\ln\frac{\mu^2}{m_i^2}\right], \end{aligned} \tag{4.10}$$

where $\Gamma_i' = \partial\boldsymbol{\Gamma}_\mathbf{i}/\partial\ln\mu$, and $\boldsymbol{\Gamma}_i$ and β_i are the coefficients of the perturbative expansion of the anomalous dimensions and of the QCD beta-function, respectively (expressed in the powers of renormalised coupling constant α_s). The anomalous dimension matrix $\boldsymbol{\Gamma}$ for the $q\bar{q} \to t\bar{t}$ has been reported in [78].

4.2 Finite terms

In figure 10, we plot the finite part of one- and two-loop renormalised amplitudes $\mathcal{M}_0^{(i)}$, $i = 1, 2$ in the physical region, as function of the auxiliary kinematic variables η and ϕ, defined in eq. (2.4), by setting $n_l = 5$, $n_h = 1$, and $N_c = 3$. The contributions of the individual colour factors at one and two loops are shown in figures 11 and 12.

The plots are obtained by evaluating the analytic formulas at one and two loops with high precision on 10,500 evenly spaced grid points. The numerical evaluation of the GPLs is carried out by HandyG [59] (away from threshold) and Ginac [58] (close to threshold) through their interface to PolyLogTools [57].

The numerical evaluation of the analytic expressions were carried out on a desktop machine with processor Ryzen 7 PRO 4750G and 32 GB of RAM, in which we experienced a CPU time per phase-space point ranging from $\mathcal{O}(20'')$ (within HandyG) to $\mathcal{O}(5')$

JHEP09(2022)129

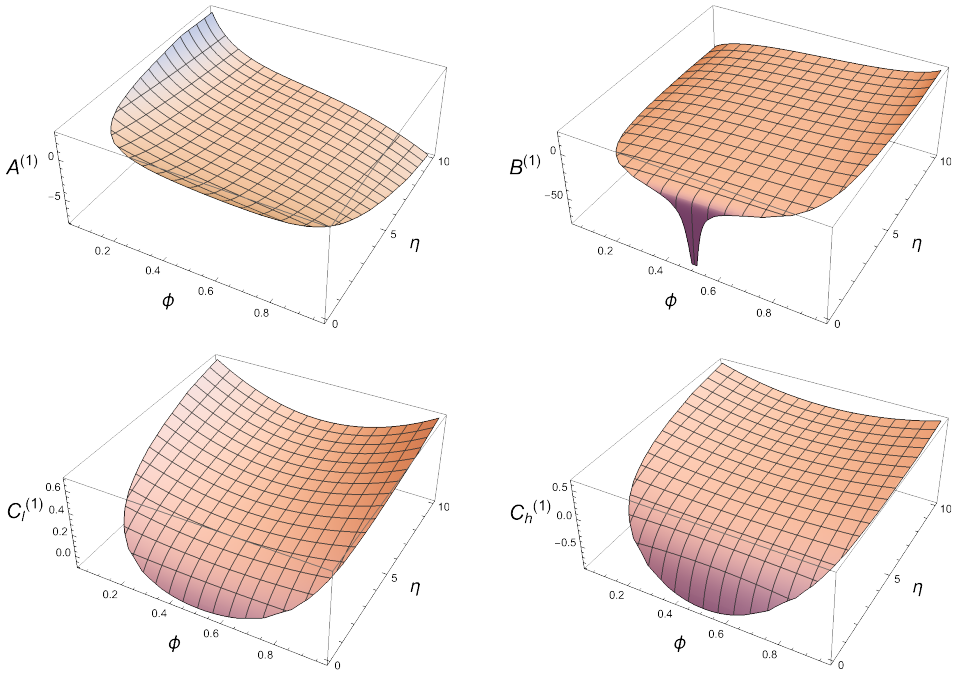

Figure 11. Three-dimensional plots of the coefficients (finite part) appearing in the decomposition of the renormalised one-loop amplitude in eq. (2.9).

(within PolyLogTools), through a setup given by Mathematica interfaces. Additionally, we observed a noteworthy feature in the region $s \gg M^2$, where the evaluation time considerably got reduced by factor of 5.

The *finite term* of the analytic expression of the two-loop contribution $\mathcal{M}_0^{(2)}$, which constitutes the main result of this communication, is found in agreement with the numerical results available in [36]. In particular, the numerical values of the grid attached to the arXiv submission of the latter reference agree with the (higher accuracy) values obtained from the numerical evaluation of our analytic expressions, in the same phase-space points. For completeness, the values of $\mathcal{M}_0^{(2)}$, numerically evaluated at 1600 phase-space points, are given in the ancillary file `qqQQGrid.m`, attached to the arXiv submission. Our grid is given in the format $\{\phi, \eta, \mathcal{M}_0^{(2)}\}$, for the scale choice $\mu^2 = M^2$, in the same phase-space points chosen in [36].

In table 1, we showcase the numerical values of the analytic expressions of the individual colour factors, at one- and two-loop. The analytic expressions are evaluated with Ginac at the kinematic point $s/M^2 = 5$, $t/M^2 = -5/4$, $\mu^2 = M^2$ (following the prescription given in eq. (4.6), the imaginary term is chosen to have $\delta = 10^{-25}$), which corresponds to the same kinematic point as in the table 3 of [36] (see also table 1 of [37]), and our results are in agreement up-to the digits reported in the latter.

Moreover, the analytic expressions of the finite part , as well as of the poles, of $A^{(2)}$, $D_l^{(2)}$, $D_h^{(2)}$, $E_l^{(2)}$, $E_h^{(2)}$, $F_l^{(2)}$, $F_{lh}^{(2)}$, $F_h^{(2)}$ agree with earlier results published in [39, 40].

JHEP09(2022)129

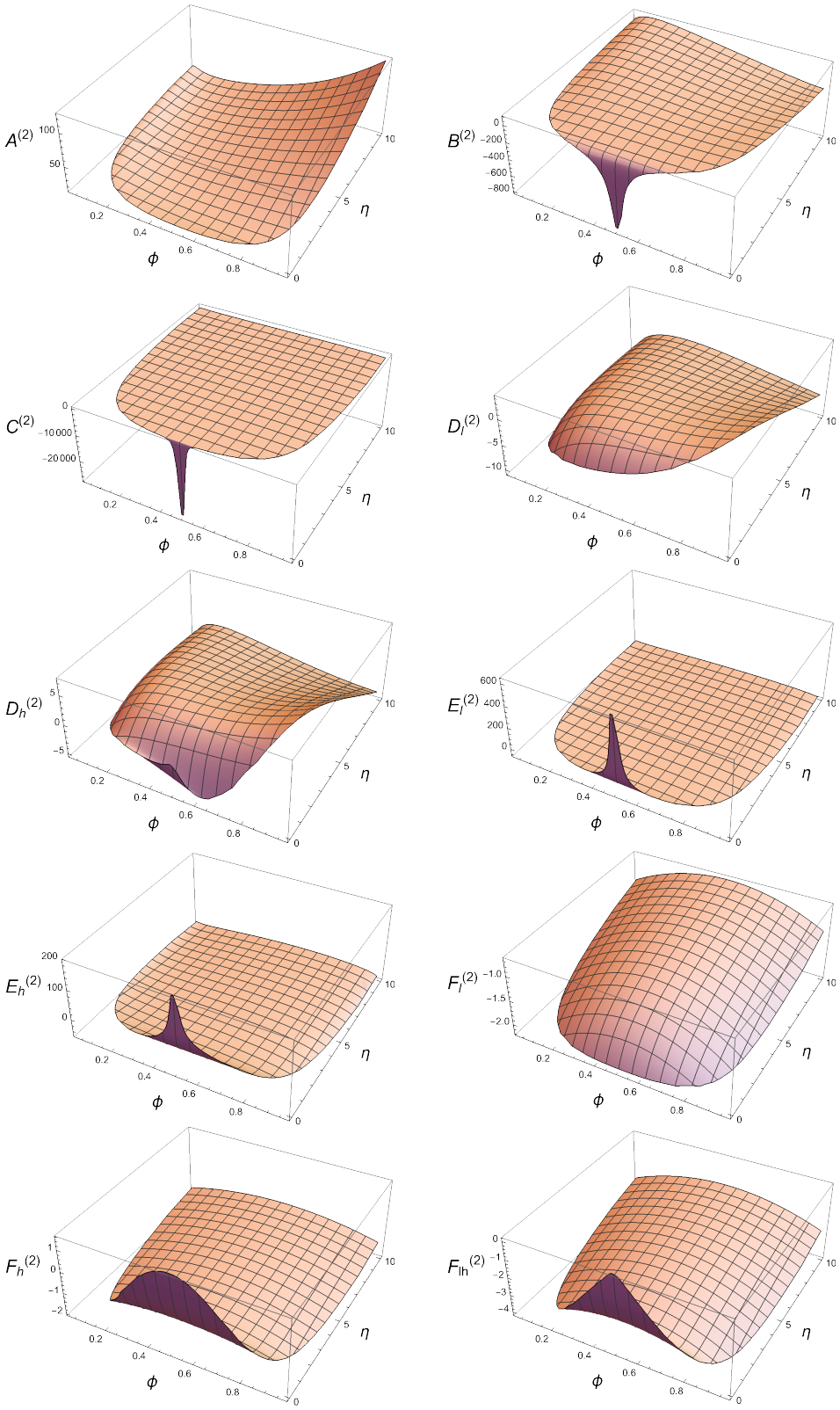

Figure 12. Three-dimensional plots of the coefficients (finite part) appearing in the decomposition of the renormalised two-loop amplitude in eq. (2.10).

JHEP09(2022)129

	ϵ^{-4}	ϵ^{-3}	ϵ^{-2}	ϵ^{-1}	ϵ^{0}	ϵ^{1}
$A^{(0)}$	–	–	–	–	$\frac{181}{100}$	-2
$A^{(1)}$	–	–	$-\frac{181}{400}$	0.1026418456757775	1.356145770566065	2.230403451742140
$B^{(1)}$	–	–	$\frac{181}{400}$	-0.3180868339485723	-5.763132746701004	2.913169881363488
$C_l^{(1)}$	–	–	0	0	-0.01726400752682416	1.235821434465827
$C_h^{(1)}$	–	–	0	0	-0.5623350683773134	0.6373589172648111
$A^{(2)}$	$\frac{181}{800}$	1.391733154324222	-2.298174307221209	-4.145752448999165	17.37136598564062	–
$B^{(2)}$	$-\frac{181}{400}$	-1.323646320375650	8.507455541210568	6.035611156200398	-35.12861106350758	–
$C^{(2)}$	$\frac{181}{800}$	-0.06808683394857230	-18.00716652035224	6.302454931016090	3.524044912826756	–
$D_l^{(2)}$	0	$-\frac{181}{800}$	0.2605057338631945	-0.7250180282219092	-1.935417246635768	–
$D_h^{(2)}$	0	0	0.5623350683773134	0.1045606449242690	-1.704747997587188	–
$E_l^{(2)}$	0	$\frac{181}{800}$	-0.3323207299541260	7.904121951420471	2.848697836597635	–
$E_h^{(2)}$	0	0	-0.5623350683773134	4.528240788258799	12.73232424278180	–
$F_l^{(2)}$	0	0	0	0	-1.984228442234312	–
$F_{lh}^{(2)}$	0	0	0	0	-2.442562819239786	–
$F_h^{(2)}$	0	0	0	0	-0.07924540546146283	–

Table 1. Numerical values of the LO squared amplitude, in eq. (3.1), and of the coefficients appearing in the decomposition of the renormalised one- and two-loop amplitudes in eqs. (2.9) and (2.10), evaluated at the phase space point $s/M^2 = 5$, $t/M^2 = -5/4$, $\mu^2 = M^2$. The underlined digits show the agreement with the results reported in table 1 of [37].

JHEP09(2022)129

5 Conclusion

We completed the analytic evaluation of the scattering amplitude for the process $q\bar{q} \to Q\bar{Q}$ at two loops in QCD, for a massless (q) and a massive (Q) quark type. The contribution of the leading colour diagrams and of those containing fermion loops, whose analytical results were already available in the literature, were independently evaluated and cross checked, and combined with the novel contributions of the sub-leading colour terms, which were evaluated in this work, for the first time.

The un-renormalised interference terms of the one- and two-loop bare amplitudes with the leading-order one were computed in the framework of CDR. The renormalisation of the ultraviolet divergences was carried out by employing the on-shell scheme for the quarks, and the $\overline{\text{MS}}$-scheme for the strong coupling constants.

The analytic results of the one- and two-loop renormalised contributions, obtained as Laurent series around $d = 4$ dimensions, respectively, up-to the first order term, and up-to the finite term, were expressed in terms of GPLs and transcendental constants of up-to weight four. The singularity structure of the renormalised results was found to be in compliance with the predicted universal infrared behaviour of QCD amplitudes [76–78]. Numerical and partial analytical results of the scattering amplitude already available in the literature [36, 37, 39, 40] agree with the novel analytic expression.

The analytic results of the two-loop scattering amplitude for the top-quark pair production from the light-quark annihilation channel are an essential ingredient to be combined with the ones of the gluon fusion channel, whose analytic knowledge is partially available [41–44, 46, 47], to obtain – hopefully, in a not-so-far future – the full analytic expressions of the scattering amplitudes for the production of a heavy quark-antiquark pair in hadron collisions, at two loops in QCD [36, 37].

The results presented for the process $q\bar{q} \to Q\bar{Q}$ in QCD can be considered as an extension to the non-Abelian case of the ones recently obtained for the process $e^+e^- \to \mu^+\mu^-$ in QED [79]. The automatic framework which was developed for these calculations is flexible and applicable to other scattering reactions. The computational efforts and the intermediate results for the non-Abelian case, such as diagram generation, integral and integrand decompositions, and evaluation of master integrals, are ingredients that are now available for the study of the elastic scattering processes of one massless and one massive particle/body, which is related by crossing symmetry to the one presented here.

The competences acquired during this work, as well as the building blocks of the calculations, are not limited to applications within Particle Physics, and could be applied, for instance, to investigate processes in General Relativity, like the bending of light caused by a massive astrophysical body, see for instance [106, 107], where the massless quark is replaced by a photon, the massive quark is replaced by the world-line of a black-hole, and gluons are replaced by gravitons.

Let us finally remark that, more generally, the presented results constitute a crucial reference for the study of the scattering of particles/bodies with non-vanishing masses, for interactions mediated by self-interacting massless quanta, in the limiting case when one of the body can be treated as massless. Therefore, they can offer additional insights

JHEP09(2022)129

for investigating similarities and differences between fundamental interactions occurring in different physical scenarios.

Acknowledgments

We wish to thank A. Primo for collaboration at early stage of this project, in particular, during the development of Aida and for discussions on the diagrams shown in figure 6. W.J.T. would like to thank J. Mazzitelli for suggesting numerical checks on the analytic expressions presented in this manuscript. We wish to acknowledge R. Bonciani, A. Broggio, M. Czakon, S. Di Vita, A. Ferroglia, F. Gasparotto, T. Gehrmann, M. Grazzini, A. Primo, U. Schubert, A. Signer, and F. Tramontano, for stimulating discussions at various stages, and comments on the manuscript. The work of M.K.M is supported by Fellini - Fellowship for Innovation at INFN funded by the European Union's Horizon 2020 research and innovation programme under the Marie Skłodowska-Curie grant agreement No 754496. J.R. acknowledges support from INFN. This project received funding from the European Research Council (ERC) under the European Union's Horizon 2020 research and innovation programme (grant agreement No 725110), *Novel structures in scattering amplitudes.*

A Colour stripped form factors

The Feynman diagrammatic approach has been adopted throughout the calculation, and in this appendix, we provide details on the contribution of the one- and two-loop Feynman diagrams to the form factors present in decompositions (2.9) and (2.10), respectively.

In decomposition (2.9), for the one-loop contribution, we need to deal with 10 non-vanishing Feynman diagrams (see figure 2). Two of them contain vacuum polarisation insertions (with a closed heavy- and light-quark loop) contributing to form factors $C_l^{(1)}$ and $C_h^{(1)}$. The remaining 8 diagrams may contribute to either $A^{(1)}$ (5 diagrams) or $B^{(1)}$ (4 diagrams). In particular, $A^{(1)}$ gets contribution from purely planar diagrams with and without self-gluon interactions. $B^{(1)}, C_l^{(1)}$, and $C_h^{(1)}$ get contribution only from diagrams without self-gluon interactions.

Therefore, some of the form factors appearing in the decomposition of the considered amplitude, for a non-Abelian theory, can be written as linear combination of colour-stripped diagrams that would contribute to the scattering amplitude of an Abelian theory (like $e^+e^- \to \mu^+\mu^-$ in QED). We list here, the decomposition of the form factors in terms of colour-stripped (Abelian-like) diagrams:

$$\begin{aligned} B^{(1)} &= -\mathrm{d}_1^{(1)} - \mathrm{d}_3^{(1)} - 2\mathrm{d}_5^{(1)} - 2\mathrm{d}_6^{(1)}\,, \\ C_l^{(1)} &= \mathrm{d}_7^{(1)}\,, \\ C_h^{(1)} &= \mathrm{d}_8^{(1)}\,, \end{aligned} \tag{A.1}$$

where $\mathrm{d}_k^{(1)}$ accounts for colour-stripped k-th Feynman diagram of figure 2.

Similarly, the form-factors appearing in decomposition of the two-loop amplitude in (2.10), gets contribution from 184 non-vanishing Feynman diagrams. In particular: $A^{(2)}$

JHEP09(2022)129

gets contributions from 49 diagrams, which similarly to $A^{(1)}$, are only planar; $B^{(2)}$ gets contributions from 62 (planar and non-planar) diagrams; $C^{(2)}$ gets contributions from 35 (planar and non-planar) diagrams; $D_l^{(2)}$, from 19 diagrams; $D_h^{(2)}$, from 20 diagrams; $E_l^{(2)}$, from 15 diagrams; $E_h^{(2)}$, from 15 diagrams; $F_h^{(2)}$, from 1 diagram; $F_{lh}^{(2)}$, from 2 diagrams; and $F_l^{(2)}$, from 1 diagrams.

In the same way, as in the one-loop decomposition, we notice that form factors $A^{(2)}, B^{(2)}$, $D_l^{(2)}$ and $D_h^{(2)}$ get contributions from Feynman diagrams with and without self-gluon interactions, whereas, $C^{(2)}, E_l^{(2)}, E_h^{(2)}, F_l^{(2)}, F_{lh}^{(2)}$, and $F_h^{(2)}$ contain only diagrams without self-gluon interaction. Thus, the latter form factors can be decomposed in colour-stripped (Abelian-like) diagrams as:

$$
\begin{aligned}
C^{(2)} =& \,\mathrm{d}_4^{(2)} + \mathrm{d}_{12}^{(2)} + \mathrm{d}_{17}^{(2)} + \mathrm{d}_{21}^{(2)} + \mathrm{d}_{29}^{(2)} + \mathrm{d}_{34}^{(2)} + \mathrm{d}_{38}^{(2)} + 2\mathrm{d}_{42}^{(2)} + 3\mathrm{d}_{44}^{(2)} + 3\mathrm{d}_{45}^{(2)} + 2\mathrm{d}_{46}^{(2)} \\
&+ 2\mathrm{d}_{48}^{(2)} + 2\mathrm{d}_{49}^{(2)} + 2\mathrm{d}_{51}^{(2)} + 2\mathrm{d}_{53}^{(2)} + 2\mathrm{d}_{54}^{(2)} + 2\mathrm{d}_{56}^{(2)} + 2\mathrm{d}_{58}^{(2)} + 2\mathrm{d}_{60}^{(2)} + 2\mathrm{d}_{62}^{(2)} \\
&+ 3\mathrm{d}_{64}^{(2)} + 3\mathrm{d}_{65}^{(2)} + 2\mathrm{d}_{66}^{(2)} + 3\mathrm{d}_{68}^{(2)} + 3\mathrm{d}_{69}^{(2)} + \mathrm{d}_{106}^{(2)} + \mathrm{d}_{107}^{(2)} + \mathrm{d}_{112}^{(2)} + \mathrm{d}_{130}^{(2)} \\
&+ \mathrm{d}_{131}^{(2)} + \mathrm{d}_{136}^{(2)} + 2\mathrm{d}_{158}^{(2)} + 2\mathrm{d}_{163}^{(2)} + 2\mathrm{d}_{164}^{(2)} + 2\mathrm{d}_{165}^{(2)}\,, \\
E_{\mathrm{l}}^{(2)} =& -2\mathrm{d}_8^{(2)} - 2\mathrm{d}_{10}^{(2)} - 2\mathrm{d}_{25}^{(2)} - 2\mathrm{d}_{27}^{(2)} - \mathrm{d}_{78}^{(2)} - \mathrm{d}_{88}^{(2)} - \mathrm{d}_{90}^{(2)} - \mathrm{d}_{98}^{(2)} \\
&- \mathrm{d}_{117}^{(2)} - \mathrm{d}_{122}^{(2)} - \mathrm{d}_{141}^{(2)} - 2\mathrm{d}_{146}^{(2)} - 2\mathrm{d}_{150}^{(2)} - 2\mathrm{d}_{154}^{(2)} - 2\mathrm{d}_{159}^{(2)}\,, \\
E_{\mathrm{h}}^{(2)} =& -2\mathrm{d}_9^{(2)} - 2\mathrm{d}_{11}^{(2)} - 2\mathrm{d}_{26}^{(2)} - 2\mathrm{d}_{28}^{(2)} - \mathrm{d}_{79}^{(2)} - \mathrm{d}_{89}^{(2)} - \mathrm{d}_{91}^{(2)} - \mathrm{d}_{99}^{(2)} \\
&- \mathrm{d}_{118}^{(2)} - \mathrm{d}_{123}^{(2)} - \mathrm{d}_{142}^{(2)} - 2\mathrm{d}_{147}^{(2)} - 2\mathrm{d}_{151}^{(2)} - 2\mathrm{d}_{155}^{(2)} - 2\mathrm{d}_{160}^{(2)}\,, \\
F_{\mathrm{l}}^{(2)} =& \,\mathrm{d}_{168}^{(2)}\,, \\
F_{\mathrm{lh}}^{(2)} =& \,\mathrm{d}_{169}^{(2)} + \mathrm{d}_{170}^{(2)}\,, \\
F_{\mathrm{h}}^{(2)} =& \,\mathrm{d}_{171}^{(2)}\,,
\end{aligned}
\tag{A.2}
$$

with $\mathrm{d}_k^{(2)}$ stands for the colour-stripped k-th Feynman diagram of figures 3 and 4.

B Renormalisation constants

In this appendix, we provide the expressions of the UV renormalisation constants introduced in section 3.1, for convenience:

- Light quark field:

$$\delta Z_q^{(1)} = 0\,; \tag{B.1}$$

$$\delta Z_q^{(2)} = C_f T_f\, n_h \left(\frac{1}{16\epsilon} + \frac{1}{8}L_\mu - \frac{5}{96}\right)\,; \tag{B.2}$$

- Heavy quark field and mass:

$$
\begin{aligned}
\delta Z_Q^{(1)} = C_f \Bigg(&-\frac{3}{4\epsilon} - 1 - \frac{3}{4}L_\mu + \epsilon\left(-2 - L_\mu - \frac{3}{8}L_\mu^2 - \frac{\pi^2}{16}\right) \\
&+\epsilon^2\left(-4 - 2L_\mu - \frac{1}{2}L_\mu^2 - \frac{1}{8}L_\mu^3 - \frac{\pi^2}{12} - \frac{\pi^2}{16}L_\mu + \frac{1}{4}\zeta_3\right)\Bigg)\,;
\end{aligned}
\tag{B.3}
$$

JHEP09(2022)129

$$\delta Z_Q^{(2)} = C_f T_f\, n_h\Big(\frac{1}{16\epsilon}+\frac{1}{4\epsilon}L_\mu+\frac{947}{288}+\frac{11}{24}L_\mu+\frac{3}{8}L_\mu^2-\frac{5\pi^2}{16}\Big) \tag{B.4}$$
$$+C_f T_f\, n_l\Big(-\frac{1}{8\epsilon^2}+\frac{11}{48\epsilon}+\frac{113}{96}+\frac{19}{24}L_\mu+\frac{1}{8}L_\mu^2+\frac{\pi^2}{12}\Big)$$
$$+C_f^2\Big(\frac{9}{32\epsilon^2}+\frac{51}{64\epsilon}+\frac{9}{16\epsilon}L_\mu+\frac{433}{128}+\frac{51}{32}L_\mu+\frac{9}{16}L_\mu^2-\frac{49\pi^2}{64}+\pi^2\ln(2)-\frac{3\zeta_3}{2}\Big)$$
$$+C_f C_A\Big(\frac{11}{32\epsilon^2}-\frac{127}{192\epsilon}-\frac{1705}{384}-\frac{215}{96}L_\mu-\frac{11}{32}L_\mu^2+\frac{5\pi^2}{16}-\frac{\pi^2\ln(2)}{2}+3\zeta_3\Big)\,;$$
$$\delta Z_M^{(1)} = C_f\Big(-\frac{3}{4\epsilon}-1-\frac{3}{4}L_\mu+\epsilon\Big(-2-L_\mu-\frac{3}{8}L_\mu^2-\frac{\pi^2}{16}\Big)$$
$$+\epsilon^2\Big(-4-2L_\mu-\frac{1}{2}L_\mu^2-\frac{1}{8}L_\mu^3-\frac{\pi^2}{12}-\frac{\pi^2}{16}L_\mu+\frac{1}{4}\zeta_3\Big)\Big); \tag{B.5}$$

- Coupling constant:

$$\delta Z_{\alpha_s}^{(1)} = \Big(-\frac{11}{12\epsilon}C_A+\frac{1}{3\epsilon}T_f\,(n_l+n_h)\Big)\,; \tag{B.6}$$
$$\delta Z_{\alpha_s}^{(2)} = C_A^2\Big(\frac{121}{144\epsilon^2}-\frac{17}{48\epsilon}\Big)+C_A T_f(n_l+n_h)\Big(\frac{5}{24\epsilon}-\frac{11}{18\epsilon^2}\Big)$$
$$+C_f T_f(n_l+n_h)\frac{1}{8\epsilon}+T_f^2\,(n_l+n_h)^2\,\frac{1}{9\epsilon^2}\,; \tag{B.7}$$

  where $L_\mu \equiv \ln(\mu^2/M^2)$.

References

[1] P. Nason, S. Dawson and R.K. Ellis, *The total cross-section for the production of heavy quarks in hadronic collisions*, *Nucl. Phys. B* **303** (1988) 607 [INSPIRE].

[2] W. Beenakker, H. Kuijf, W.L. van Neerven and J. Smith, *QCD corrections to heavy quark production in $p\bar{p}$ collisions*, *Phys. Rev. D* **40** (1989) 54 [INSPIRE].

[3] W. Beenakker, W.L. van Neerven, R. Meng, G.A. Schuler and J. Smith, *QCD corrections to heavy quark production in hadron hadron collisions*, *Nucl. Phys. B* **351** (1991) 507 [INSPIRE].

[4] P. Nason, S. Dawson and R.K. Ellis, *The one particle inclusive differential cross-section for heavy quark production in hadronic collisions*, *Nucl. Phys. B* **327** (1989) 49 [*Erratum ibid.* **335** (1990) 260] [INSPIRE].

[5] M. Czakon and A. Mitov, *Inclusive heavy flavor hadroproduction in NLO QCD: the exact analytic result*, *Nucl. Phys. B* **824** (2010) 111 [arXiv:0811.4119] [INSPIRE].

[6] P. Bärnreuther, M. Czakon and A. Mitov, *Percent level precision physics at the tevatron: first genuine NNLO QCD corrections to $q\bar{q} \to t\bar{t}+X$*, *Phys. Rev. Lett.* **109** (2012) 132001 [arXiv:1204.5201] [INSPIRE].

JHEP09(2022)129

[7] M. Czakon and A. Mitov, *NNLO corrections to top-pair production at hadron colliders: the all-fermionic scattering channels*, *JHEP* **12** (2012) 054 [arXiv:1207.0236] [INSPIRE].

[8] M. Czakon and A. Mitov, *NNLO corrections to top pair production at hadron colliders: the quark-gluon reaction*, *JHEP* **01** (2013) 080 [arXiv:1210.6832] [INSPIRE].

[9] M. Czakon, P. Fiedler and A. Mitov, *Total top-quark pair-production cross section at hadron colliders through* $O(\alpha_S^4)$, *Phys. Rev. Lett.* **110** (2013) 252004 [arXiv:1303.6254] [INSPIRE].

[10] A. Gehrmann-De Ridder, T. Gehrmann and E.W.N. Glover, *Antenna subtraction at NNLO*, *JHEP* **09** (2005) 056 [hep-ph/0505111] [INSPIRE].

[11] G. Abelof and A. Gehrmann-De Ridder, *Antenna subtraction for the production of heavy particles at hadron colliders*, *JHEP* **04** (2011) 063 [arXiv:1102.2443] [INSPIRE].

[12] G. Abelof, A. Gehrmann-De Ridder, P. Maierhofer and S. Pozzorini, *NNLO QCD subtraction for top-antitop production in the* $q\bar{q}$ *channel*, *JHEP* **08** (2014) 035 [arXiv:1404.6493] [INSPIRE].

[13] G. Abelof and A. Gehrmann-De Ridder, *Light fermionic NNLO QCD corrections to top-antitop production in the quark-antiquark channel*, *JHEP* **12** (2014) 076 [arXiv:1409.3148] [INSPIRE].

[14] G. Abelof, A. Gehrmann-De Ridder and I. Majer, *Top quark pair production at NNLO in the quark-antiquark channel*, *JHEP* **12** (2015) 074 [arXiv:1506.04037] [INSPIRE].

[15] M. Czakon, P. Fiedler and A. Mitov, *Resolving the Tevatron top quark forward-backward asymmetry puzzle: fully differential next-to-next-to-leading-order calculation*, *Phys. Rev. Lett.* **115** (2015) 052001 [arXiv:1411.3007] [INSPIRE].

[16] M. Czakon, D. Heymes and A. Mitov, *High-precision differential predictions for top-quark pairs at the LHC*, *Phys. Rev. Lett.* **116** (2016) 082003 [arXiv:1511.00549] [INSPIRE].

[17] M. Czakon, P. Fiedler, D. Heymes and A. Mitov, *NNLO QCD predictions for fully-differential top-quark pair production at the Tevatron*, *JHEP* **05** (2016) 034 [arXiv:1601.05375] [INSPIRE].

[18] M. Czakon, D. Heymes and A. Mitov, *fastNLO tables for NNLO top-quark pair differential distributions*, arXiv:1704.08551 [INSPIRE].

[19] M. Czakon, *A novel subtraction scheme for double-real radiation at NNLO*, *Phys. Lett. B* **693** (2010) 259 [arXiv:1005.0274] [INSPIRE].

[20] M. Czakon, *Double-real radiation in hadronic top quark pair production as a proof of a certain concept*, *Nucl. Phys. B* **849** (2011) 250 [arXiv:1101.0642] [INSPIRE].

[21] M. Czakon and D. Heymes, *Four-dimensional formulation of the sector-improved residue subtraction scheme*, *Nucl. Phys. B* **890** (2014) 152 [arXiv:1408.2500] [INSPIRE].

[22] R. Bonciani, S. Catani, M. Grazzini, H. Sargsyan and A. Torre, *The* q_T *subtraction method for top quark production at hadron colliders*, *Eur. Phys. J. C* **75** (2015) 581 [arXiv:1508.03585] [INSPIRE].

[23] S. Catani, S. Devoto, M. Grazzini, S. Kallweit and J. Mazzitelli, *Top-quark pair production at the LHC: fully differential QCD predictions at NNLO*, *JHEP* **07** (2019) 100 [arXiv:1906.06535] [INSPIRE].

[24] S. Catani, S. Devoto, M. Grazzini, S. Kallweit, J. Mazzitelli and H. Sargsyan, *Top-quark pair hadroproduction at next-to-next-to-leading order in QCD*, *Phys. Rev. D* **99** (2019) 051501 [arXiv:1901.04005] [INSPIRE].

JHEP09(2022)129

[25] S. Catani, S. Devoto, M. Grazzini, S. Kallweit and J. Mazzitelli, *Top-quark pair hadroproduction at NNLO: differential predictions with the $\overline{MS}$ mass*, *JHEP* **08** (2020) 027 [arXiv:2005.00557] [INSPIRE].

[26] S. Catani, S. Devoto, M. Grazzini, S. Kallweit and J. Mazzitelli, *Bottom-quark production at hadron colliders: fully differential predictions in NNLO QCD*, *JHEP* **03** (2021) 029 [arXiv:2010.11906] [INSPIRE].

[27] S. Catani and M. Grazzini, *An NNLO subtraction formalism in hadron collisions and its application to Higgs boson production at the LHC*, *Phys. Rev. Lett.* **98** (2007) 222002 [hep-ph/0703012] [INSPIRE].

[28] W.J. Torres Bobadilla et al., *May the four be with you: Novel IR-subtraction methods to tackle NNLO calculations*, *Eur. Phys. J. C* **81** (2021) 250 [arXiv:2012.02567] [INSPIRE].

[29] G. Heinrich, *Collider physics at the precision frontier*, *Phys. Rept.* **922** (2021) 1 [arXiv:2009.00516] [INSPIRE].

[30] S. Dittmaier, P. Uwer and S. Weinzierl, *NLO QCD corrections to $t\bar{t}$ + jet production at hadron colliders*, *Phys. Rev. Lett.* **98** (2007) 262002 [hep-ph/0703120] [INSPIRE].

[31] S. Dittmaier, P. Uwer and S. Weinzierl, *Hadronic top-quark pair production in association with a hard jet at next-to-leading order QCD: Phenomenological studies for the Tevatron and the LHC*, *Eur. Phys. J. C* **59** (2009) 625 [arXiv:0810.0452] [INSPIRE].

[32] S. Badger, M. Becchetti, E. Chaubey, R. Marzucca and F. Sarandrea, *One-loop QCD helicity amplitudes for $pp \to t\bar{t}j$ to $O(\varepsilon^2)$*, *JHEP* **06** (2022) 066 [arXiv:2201.12188] [INSPIRE].

[33] J.G. Korner, Z. Merebashvili and M. Rogal, *NNLO $O(\alpha_s^4)$ results for heavy quark pair production in quark-antiquark collisions: the one-loop squared contributions*, *Phys. Rev. D* **77** (2008) 094011 [*Erratum ibid.* **85** (2012) 119904] [arXiv:0802.0106] [INSPIRE].

[34] C. Anastasiou and S.M. Aybat, *The one-loop gluon amplitude for heavy-quark production at NNLO*, *Phys. Rev. D* **78** (2008) 114006 [arXiv:0809.1355] [INSPIRE].

[35] B. Kniehl, Z. Merebashvili, J.G. Korner and M. Rogal, *Heavy quark pair production in gluon fusion at next-to-next-to-leading $O(\alpha_s^{4)}$ order: One-loop squared contributions*, *Phys. Rev. D* **78** (2008) 094013 [arXiv:0809.3980] [INSPIRE].

[36] M. Czakon, *Tops from light quarks: full mass dependence at two-loops in QCD*, *Phys. Lett. B* **664** (2008) 307 [arXiv:0803.1400] [INSPIRE].

[37] P. Bärnreuther, M. Czakon and P. Fiedler, *Virtual amplitudes and threshold behaviour of hadronic top-quark pair-production cross sections*, *JHEP* **02** (2014) 078 [arXiv:1312.6279] [INSPIRE].

[38] L. Chen, M. Czakon and R. Poncelet, *Polarized double-virtual amplitudes for heavy-quark pair production*, *JHEP* **03** (2018) 085 [arXiv:1712.08075] [INSPIRE].

[39] R. Bonciani, A. Ferroglia, T. Gehrmann, D. Maître and C. Studerus, *Two-loop fermionic corrections to heavy-quark pair production: the quark-antiquark channel*, *JHEP* **07** (2008) 129 [arXiv:0806.2301] [INSPIRE].

[40] R. Bonciani, A. Ferroglia, T. Gehrmann and C. Studerus, *Two-loop planar corrections to heavy-quark pair production in the quark-antiquark channel*, *JHEP* **08** (2009) 067 [arXiv:0906.3671] [INSPIRE].

JHEP09(2022)129

[41] R. Bonciani, A. Ferroglia, T. Gehrmann, A. von Manteuffel and C. Studerus, *Two-loop leading color corrections to heavy-quark pair production in the gluon fusion channel*, *JHEP* **01** (2011) 102 [arXiv:1011.6661] [INSPIRE].

[42] A. von Manteuffel and C. Studerus, *Massive planar and non-planar double box integrals for light N_f contributions to $gg \to tt$*, *JHEP* **10** (2013) 037 [arXiv:1306.3504] [INSPIRE].

[43] R. Bonciani, A. Ferroglia, T. Gehrmann, A. von Manteuffel and C. Studerus, *Light-quark two-loop corrections to heavy-quark pair production in the gluon fusion channel*, *JHEP* **12** (2013) 038 [arXiv:1309.4450] [INSPIRE].

[44] S. Badger, E. Chaubey, H.B. Hartanto and R. Marzucca, *Two-loop leading colour QCD helicity amplitudes for top quark pair production in the gluon fusion channel*, *JHEP* **06** (2021) 163 [arXiv:2102.13450] [INSPIRE].

[45] M. Czakon, A. Mitov and S. Moch, *Heavy-quark production in gluon fusion at two loops in QCD*, *Nucl. Phys. B* **798** (2008) 210 [arXiv:0707.4139] [INSPIRE].

[46] L. Adams, E. Chaubey and S. Weinzierl, *Planar double box integral for top pair production with a closed top loop to all orders in the dimensional regularization parameter*, *Phys. Rev. Lett.* **121** (2018) 142001 [arXiv:1804.11144] [INSPIRE].

[47] L. Adams, E. Chaubey and S. Weinzierl, *Analytic results for the planar double box integral relevant to top-pair production with a closed top loop*, *JHEP* **10** (2018) 206 [arXiv:1806.04981] [INSPIRE].

[48] M. Czakon, A. Mitov and S. Moch, *Heavy-quark production in massless quark scattering at two loops in QCD*, *Phys. Lett. B* **651** (2007) 147 [arXiv:0705.1975] [INSPIRE].

[49] P. Mastrolia, T. Peraro, A. Primo, J. Ronca and W.J. Torres Bobadilla, *AIDA, Adaptive Integrand Decomposition Algorithm*, (2019).

[50] P. Mastrolia, T. Peraro and A. Primo, *Adaptive Integrand Decomposition in parallel and orthogonal space*, *JHEP* **08** (2016) 164 [arXiv:1605.03157] [INSPIRE].

[51] P. Mastrolia, T. Peraro, A. Primo and W.J. Torres Bobadilla, *Adaptive Integrand Decomposition*, *PoS* **LL2016** (2016) 007 [arXiv:1607.05156] [INSPIRE].

[52] T. Hahn, *Generating Feynman diagrams and amplitudes with FeynArts 3*, *Comput. Phys. Commun.* **140** (2001) 418 [hep-ph/0012260] [INSPIRE].

[53] V. Shtabovenko, R. Mertig and F. Orellana, *New developments in FeynCalc 9.0*, *Comput. Phys. Commun.* **207** (2016) 432 [arXiv:1601.01167] [INSPIRE].

[54] A. von Manteuffel and C. Studerus, *Reduze 2 — Distributed Feynman Integral Reduction*, arXiv:1201.4330 [INSPIRE].

[55] P. Maierhöfer, J. Usovitsch and P. Uwer, *Kira — A Feynman integral reduction program*, *Comput. Phys. Commun.* **230** (2018) 99 [arXiv:1705.05610] [INSPIRE].

[56] S. Borowka, G. Heinrich, S.P. Jones, M. Kerner, J. Schlenk and T. Zirke, *SecDec-3.0: numerical evaluation of multi-scale integrals beyond one loop*, *Comput. Phys. Commun.* **196** (2015) 470 [arXiv:1502.06595] [INSPIRE].

[57] C. Duhr and F. Dulat, *PolyLogTools — Polylogs for the masses*, *JHEP* **08** (2019) 135 [arXiv:1904.07279] [INSPIRE].

[58] J. Vollinga and S. Weinzierl, *Numerical evaluation of multiple polylogarithms*, *Comput. Phys. Commun.* **167** (2005) 177 [hep-ph/0410259] [INSPIRE].

JHEP09(2022)129

[59] L. Naterop, A. Signer and Y. Ulrich, *handyG — Rapid numerical evaluation of generalised polylogarithms in Fortran*, *Comput. Phys. Commun.* **253** (2020) 107165 [arXiv:1909.01656].

[60] T. Gehrmann and E. Remiddi, *Differential equations for two loop four point functions*, *Nucl. Phys. B* **580** (2000) 485 [hep-ph/9912329] [INSPIRE].

[61] R. Bonciani, P. Mastrolia and E. Remiddi, *Vertex diagrams for the QED form-factors at the two loop level*, *Nucl. Phys. B* **661** (2003) 289 [*Erratum ibid.* **702** (2004) 359] [hep-ph/0301170] [INSPIRE].

[62] R. Bonciani, P. Mastrolia and E. Remiddi, *Master integrals for the two loop QCD virtual corrections to the forward backward asymmetry*, *Nucl. Phys. B* **690** (2004) 138 [hep-ph/0311145] [INSPIRE].

[63] P. Mastrolia, M. Passera, A. Primo and U. Schubert, *Master integrals for the NNLO virtual corrections to μe scattering in QED: the planar graphs*, *JHEP* **11** (2017) 198 [arXiv:1709.07435] [INSPIRE].

[64] S. Di Vita, T. Gehrmann, S. Laporta, P. Mastrolia, A. Primo and U. Schubert, *Master integrals for the NNLO virtual corrections to $q\bar{q} \to t\bar{t}$ scattering in QCD: the non-planar graphs*, *JHEP* **06** (2019) 117 [arXiv:1904.10964] [INSPIRE].

[65] M. Becchetti, R. Bonciani, V. Casconi, A. Ferroglia, S. Lavacca and A. von Manteuffel, *Master Integrals for the two-loop, non-planar QCD corrections to top-quark pair production in the quark-annihilation channel*, *JHEP* **08** (2019) 071 [arXiv:1904.10834] [INSPIRE].

[66] S. Catani, *The singular behavior of QCD amplitudes at two loop order*, *Phys. Lett. B* **427** (1998) 161 [hep-ph/9802439] [INSPIRE].

[67] G.F. Sterman and M.E. Tejeda-Yeomans, *Multiloop amplitudes and resummation*, *Phys. Lett. B* **552** (2003) 48 [hep-ph/0210130] [INSPIRE].

[68] S.M. Aybat, L.J. Dixon and G.F. Sterman, *The Two-loop soft anomalous dimension matrix and resummation at next-to-next-to leading pole*, *Phys. Rev. D* **74** (2006) 074004 [hep-ph/0607309] [INSPIRE].

[69] S.M. Aybat, L.J. Dixon and G.F. Sterman, *The two-loop anomalous dimension matrix for soft gluon exchange*, *Phys. Rev. Lett.* **97** (2006) 072001 [hep-ph/0606254] [INSPIRE].

[70] E. Gardi and L. Magnea, *Factorization constraints for soft anomalous dimensions in QCD scattering amplitudes*, *JHEP* **03** (2009) 079 [arXiv:0901.1091] [INSPIRE].

[71] E. Gardi and L. Magnea, *Infrared singularities in QCD amplitudes*, *Nuovo Cim. C* **32N5-6** (2009) 137 [arXiv:0908.3273] [INSPIRE].

[72] T. Becher and M. Neubert, *Infrared singularities of scattering amplitudes in perturbative QCD*, *Phys. Rev. Lett.* **102** (2009) 162001 [*Erratum ibid.* **111** (2013) 199905] [arXiv:0901.0722] [INSPIRE].

[73] T. Becher and M. Neubert, *Infrared singularities of scattering amplitudes and N^3LL resummation for n-jet processes*, *JHEP* **01** (2020) 025 [arXiv:1908.11379] [INSPIRE].

[74] T. Becher and M. Neubert, *On the structure of infrared singularities of gauge-theory amplitudes*, *JHEP* **06** (2009) 081 [*Erratum ibid.* **11** (2013) 024] [arXiv:0903.1126] [INSPIRE].

[75] A. Mitov and S. Moch, *The singular behavior of massive QCD amplitudes*, *JHEP* **05** (2007) 001 [hep-ph/0612149] [INSPIRE].

JHEP09(2022)129

[76] T. Becher and M. Neubert, *Infrared singularities of QCD amplitudes with massive partons*, *Phys. Rev. D* **79** (2009) 125004 [*Erratum ibid.* **80** (2009) 109901] [arXiv:0904.1021] [INSPIRE].

[77] A. Ferroglia, M. Neubert, B.D. Pecjak and L.L. Yang, *Two-loop divergences of scattering amplitudes with massive partons*, *Phys. Rev. Lett.* **103** (2009) 201601 [arXiv:0907.4791] [INSPIRE].

[78] A. Ferroglia, M. Neubert, B.D. Pecjak and L.L. Yang, *Two-loop divergences of massive scattering amplitudes in non-abelian gauge theories*, *JHEP* **11** (2009) 062 [arXiv:0908.3676] [INSPIRE].

[79] R. Bonciani et al., *Two-loop four-fermion scattering amplitude in QED*, *Phys. Rev. Lett.* **128** (2022) 022002 [arXiv:2106.13179] [INSPIRE].

[80] J. Mazzitelli, P.F. Monni, P. Nason, E. Re, M. Wiesemann and G. Zanderighi, *Next-to-next-to-leading order event generation for top-quark pair production*, *Phys. Rev. Lett.* **127** (2021) 062001 [arXiv:2012.14267] [INSPIRE].

[81] J. Mazzitelli, P.F. Monni, P. Nason, E. Re, M. Wiesemann and G. Zanderighi, *Top-pair production at the LHC with MINNLO$_{PS}$*, *JHEP* **04** (2022) 079 [arXiv:2112.12135] [INSPIRE].

[82] ATLAS collaboration, *Measurements of differential cross-sections in top-quark pair events with a high transverse momentum top quark and limits on beyond the Standard Model contributions to top-quark pair production with the ATLAS detector at* $\sqrt{s} = 13$ *TeV*, *JHEP* **06** (2022) 063 [arXiv:2202.12134] [INSPIRE].

[83] M.L. Mangano, P. Nason and G. Ridolfi, *Heavy quark correlations in hadron collisions at next-to-leading order*, *Nucl. Phys. B* **373** (1992) 295 [INSPIRE].

[84] J.G. Korner and Z. Merebashvili, *One loop corrections to four point functions with two external massive fermions and two external massless partons*, *Phys. Rev. D* **66** (2002) 054023 [hep-ph/0207054] [INSPIRE].

[85] W. Bernreuther, A. Brandenburg, Z.G. Si and P. Uwer, *Top quark pair production and decay at hadron colliders*, *Nucl. Phys. B* **690** (2004) 81 [hep-ph/0403035] [INSPIRE].

[86] G. 't Hooft and M.J.G. Veltman, *Regularization and renormalization of gauge fields*, *Nucl. Phys. B* **44** (1972) 189 [INSPIRE].

[87] C.G. Bollini and J.J. Giambiagi, *Dimensional renormalization: the number of dimensions as a regularizing parameter*, *Nuovo Cim. B* **12** (1972) 20 [INSPIRE].

[88] C. Gnendiger et al., *To d, or not to d: recent developments and comparisons of regularization schemes*, *Eur. Phys. J. C* **77** (2017) 471 [arXiv:1705.01827] [INSPIRE].

[89] K.G. Chetyrkin and M. Steinhauser, *Short distance mass of a heavy quark at order* α_s^3, *Phys. Rev. Lett.* **83** (1999) 4001 [hep-ph/9907509] [INSPIRE].

[90] K. Melnikov and T.v. Ritbergen, *The three loop relation between the MS-bar and the pole quark masses*, *Phys. Lett. B* **482** (2000) 99 [hep-ph/9912391] [INSPIRE].

[91] K. Melnikov and T. van Ritbergen, *The three loop on-shell renormalization of QCD and QED*, *Nucl. Phys. B* **591** (2000) 515 [hep-ph/0005131] [INSPIRE].

[92] T. van Ritbergen, J.A.M. Vermaseren and S.A. Larin, *The four loop β-function in quantum chromodynamics*, *Phys. Lett. B* **400** (1997) 379 [hep-ph/9701390] [INSPIRE].

JHEP09(2022)129

[93] M. Czakon, *The Four-loop QCD β-function and anomalous dimensions*, *Nucl. Phys. B* **710** (2005) 485 [hep-ph/0411261] [INSPIRE].

[94] P.A. Baikov, K.G. Chetyrkin and J.H. Kühn, *Five-loop running of the QCD coupling constant*, *Phys. Rev. Lett.* **118** (2017) 082002 [arXiv:1606.08659] [INSPIRE].

[95] T. Luthe, A. Maier, P. Marquard and Y. Schröder, *Towards the five-loop β-function for a general gauge group*, *JHEP* **07** (2016) 127 [arXiv:1606.08662] [INSPIRE].

[96] F. Herzog, B. Ruijl, T. Ueda, J.A.M. Vermaseren and A. Vogt, *The five-loop β-function of Yang-Mills theory with fermions*, *JHEP* **02** (2017) 090 [arXiv:1701.01404] [INSPIRE].

[97] K.G. Chetyrkin, G. Falcioni, F. Herzog and J.A.M. Vermaseren, *Five-loop renormalisation of QCD in covariant gauges*, *JHEP* **10** (2017) 179 [*Addendum ibid.* **12** (2017) 006] [arXiv:1709.08541] [INSPIRE].

[98] F.V. Tkachov, *A theorem on analytical calculability of four loop renormalization group functions*, *Phys. Lett. B* **100** (1981) 65 [INSPIRE].

[99] K.G. Chetyrkin and F.V. Tkachov, *Integration by parts: the algorithm to calculate β-functions in 4 loops*, *Nucl. Phys. B* **192** (1981) 159 [INSPIRE].

[100] S. Laporta, *High precision calculation of multiloop Feynman integrals by difference equations*, *Int. J. Mod. Phys. A* **15** (2000) 5087 [hep-ph/0102033] [INSPIRE].

[101] S. Di Vita, S. Laporta, P. Mastrolia, A. Primo and U. Schubert, *Master integrals for the NNLO virtual corrections to μe scattering in QED: the non-planar graphs*, *JHEP* **09** (2018) 016 [arXiv:1806.08241] [INSPIRE].

[102] J.M. Henn and W.J.T. Bobadilla, *Maximal transcendental weight contribution of scattering amplitudes*, *JHEP* **03** (2022) 174 [arXiv:2112.08900] [INSPIRE].

[103] M. Argeri et al., *Magnus and Dyson series for master integrals*, *JHEP* **03** (2014) 082 [arXiv:1401.2979] [INSPIRE].

[104] A.B. Goncharov, *Multiple polylogarithms, cyclotomy and modular complexes*, *Math. Res. Lett.* **5** (1998) 497 [arXiv:1105.2076] [INSPIRE].

[105] ATLAS collaboration, *Observation of a new particle in the search for the Standard Model Higgs boson with the ATLAS detector at the LHC*, *Phys. Lett. B* **716** (2012) 1 [arXiv:1207.7214] [INSPIRE].

[106] N.E.J. Bjerrum-Bohr, J.F. Donoghue, B.R. Holstein, L. Plante and P. Vanhove, *Light-like scattering in quantum gravity*, *JHEP* **11** (2016) 117 [arXiv:1609.07477] [INSPIRE].

[107] N.E.J. Bjerrum-Bohr, B.R. Holstein, J.F. Donoghue, L. Planté and P. Vanhove, *Illuminating light bending*, *PoS* **CORFU2016** (2017) 077 [arXiv:1704.01624] [INSPIRE].

JHEP09(2022)129